5G Configured Grant Scheduling for Integrated Sensing and Communication in Vehicular Networks

Veerendra Kumar Gautam*, Priyanka Nagireddy\$, Bheemarjuna Reddy Tamma\$, and C. Siva Ram Murthy\$

*Department of Information Engineering, University of Padova, Italy

\$Indian Institute of Technology Hyderabad, India
e-mail:veerendrakumar.gautam@unipd.it, sm23mtech11007@iith.ac.in, tbr@iith.ac.in, murthy@cse.iith.ac.in

Abstract-Integrated Sensing and Communications (ISAC) enhances traditional mobile network capabilities by enabling the detection of passive, non-connected objects. Latency-sensitive vehicular applications such as Augmented Reality (AR), Virtual Reality (VR), and High Definition Maps (HD Maps) can be integrated with ISAC to improve the utilization of limited wireless resources. The Configuration Grant (CG) mechanism, in 3GPP Release 16, reduces signaling overhead in Uplink (UL) by preassigning resources to UEs (vehicles). However, employing CG for ISAC can lead to incorrect assignment of transmission slots due to the aperiodic nature of ISAC sensing traffic. To address this issue, we propose a CG allocation scheme that models the interarrival times of aperiodic traffic using a Weibull distribution. A probability distribution model, implemented and evaluated using the NS-3 5G-LENA CG module, assists the radio resource scheduler by analyzing sensing arrivals within a configuration window to predict future bursts and proactively reserve UL resources for UEs (vehicles). This prediction-driven allocation significantly improves Packet Delivery Ratio (PDR) and spectral efficiency in vehicular scenarios.

Index Terms—Integrated Sensing and Communications, Configured Grant, Vehicular Applications, Machine Learning, Radio Resource Scheduling.

I. Introduction

Vehicular applications such as High Definition Maps (HD Maps), Augmented Reality (AR), Virtual Reality (VR) maps, and services enabled by Vehicle-to-Everything (V2X) networks hold great promise for enhancing road safety, reducing traffic congestion, and improving overall traffic flow efficiency. In support of these advancements, the 3GPP Release 19 work item has emphasized the integration of Integrated Sensing and Communication (ISAC) with traditional communication services [1]. ISAC enables the detection of passive objects—those not connected to the network—while maintaining broad coverage, thereby supporting a wide range of vehicular applications. In this context, 6G communication systems aim to tightly integrate V2X networks with ISAC to meet the demands of ultra-fast, highly reliable, and low-latency applications that process and exchange large volumes of data [2]. ISAC has been extensively studied in autonomous and assisted driving systems, where real-time environmental perception is essential for safety and operational efficiency.

The Society of Automotive Engineers (SAE) categorizes driving automation into six levels, ranging from fully manual

to fully autonomous systems [3]. Vehicles¹ at Level 3 and above require HD Maps with spatial resolutions of 10-20 cm or better. HD Maps provide centimeter-level accuracy of the road and surrounding environment, enabling core autonomous driving functions such as perception, localization, navigation, and decision-making [4]. The dissemination of HD Maps is facilitated through content-centric networking services, which are subject to stringent latency constraints [5]. Companies such as HERE Technologies [6], Volvo [7], and the Toyota Research Institute-Advanced Development have introduced the concept of dynamic HD Maps, referring to frequently updated real-time mapping information. Autonomous vehicles are equipped with various onboard sensors such as cameras, radars, and lidars to enhance situational awareness further. These are complemented by Onboard Units (OBUs) that enable V2X communication, allowing vehicles to interact with infrastructure (i.e, RoadSide Units (RSUs)) and each other. While these sensors provide detailed information about a vehicle's immediate surroundings, they are limited in detecting distant or occluded objects. Thus, combining advanced sensing and communication capabilities is essential for comprehensive perception.

Achieving reliable perception often requires fusing data from multiple sensors in real-time, which demands high computational power. However, OBUs typically have limited processing capacity. To overcome this, Mobile Edge Computing (MEC) has emerged as a viable solution, providing low-latency computing resources at the network edge. Unlike traditional cloud-based systems, MEC is better suited for time-sensitive vehicular applications. Recent research has explored the integration of ISAC and MEC to enhance vehicular intelligence. For example, the authors in [8] proposed an ISAC-assisted edge-intelligent V2X communication framework where vehicles offload computation tasks to edge servers co-located with RSUs, with the objective of minimizing long-term service delay through joint optimization of offloading decisions and resource allocation. Similarly, [9] introduced a collaborative sensing architecture wherein vehicles and ISAC-equipped RSUs cooperate to expand sensing range, modeled through stochastic task arrivals and communication dynamics. However, these studies primarily focus on homogeneous task offloading. In contrast, [10] investigated scenarios involving heterogeneous

¹Throughout this paper, we use vehicles and User Equipments (UEs) interchangeably.

tasks with different priorities and optimized delay-sensitive offloading strategies for MEC. While significant, these works did not explore Configured Grant (CG)—a semi-persistent scheduling method to reduce control signaling overhead in 5G based V2X systems. Recently, [11] conducted the first investigation of CG in 5G based vehicular networks, evaluating how periodic task offloading and UE mobility influence Packet Delivery Ratio (PDR) and radio resource efficiency under CG scheduling.

To the best of our knowledge, no prior work has explored the integration of CG with ISAC and HD map data offloading in vehicular networks. Our key contributions are listed below.

- Periodic HD Map Data Offloading: We study periodic HD
 map data offloading and analyze the impact of vehicular
 mobility on CG resource allocation. A Long Short-Term
 Memory (LSTM) model is trained to predict the most
 appropriate Modulation and Coding Scheme (MCS) of
 UEs, which are used for dynamic CG assignment in UL.
- Aperiodic Sensing Data Modeling: Sensing data is modeled as aperiodic traffic using the Weibull distribution to predict future occurrences based on historical observations. These predictions are combined with the LSTM model's output to improve CG allocation accuracy.
- Joint Scheduling of Heterogeneous Traffic: We simulate joint scheduling for periodic and aperiodic traffic and evaluate performance using PDR as the primary metric.

II. RELATED WORK

There has been significant research [10]-[13] focused on optimizing offloading decisions, as well as radio and computing resource allocation, in ISAC-enabled vehicular networks. Both optimization-based and Machine Learning (ML)-based approaches have been proposed and evaluated. In [10], the authors developed a Multi-Agent Deep Deterministic Policy Gradientbased Offloading Optimization and Resource Allocation Algorithm (MADDPG-O2RA2) to address a mixed-integer nonlinear programming (MINLP) problem. Their solution jointly optimizes offloading decisions and resource block allocation. Similarly [12], Deep Reinforcement Learning (DRL) approach to optimize resource allocation in 6G V2X networks, focuses on enhancing energy efficiency and transmission reliability. The DRL agent dynamically adjusts resource allocation based on real-time network states and vehicular mobility, helping reduce energy consumption while maintaining high Quality of Service (QoS). Simulation results demonstrate that the DRL-based strategy outperforms traditional baseline methods regarding energy usage, latency, and network throughput. In [13], the authors formulated a joint optimization problem for resource allocation and beamforming design aimed at minimizing system delay in the presence of heterogeneous tasks, while satisfying the quality requirements for sensing. They decomposed the original problem into two sub-problems and proposed an efficient solution approach based on alternating optimization and successive convex approximation. More recently, [11] examined the use of CG in a vehicular scenario. The study introduced a CG allocation algorithm that leverages ML techniques to predict the MCS of vehicles, thereby improving CG scheduling. Their results demonstrated notable enhancements in PDR and spectrum utilization efficiency.

Despite the contributions of these studies, none have addressed the joint use of CG for both periodic and aperiodic data offloading in high-mobility vehicular networks. In such environments, the rapid variation in channel conditions due to vehicle mobility poses a significant challenge for real-time resource allocation. To the best of our knowledge, this complex issue has not been studied in the literature. Hence, our work proposes a novel framework that applies CG-based scheduling to both HD Map (periodic) and sensing data (aperiodic) offloading in a unified manner. We aim to ensure low latency communication and efficient utilization of radio resources, while accounting for the dynamic nature of channels in vehicular networks.

III. SYSTEM MODEL

To assess the impact of CG transmission on the PDR in a 5G NR V2X network, we consider a scenario involving V vehicles, each equipped with state-of-the-art ISAC systems, operating within the coverage area of a single gNodeB. A general spectrum-sharing model is adopted, where all ISAC devices perform both radar based sensing and data transmission over the same frequency channel. Each ISAC-enabled vehicle offloads radar-sensing data to an MEC server via short-packet transmission. This enables ISAC-equipped RSUs to access real-time environmental data, thereby extending the effective sensing range of the vehicles. Each vehicle simultaneously generates two types of data in Uplink (UL): aperiodic radarsensing data and periodic HD Map data. The multi-source perception data from vehicles and their ISAC systems are processed through data fusion, yielding comprehensive situational awareness. Cooperative perception between the gNodeB and vehicles helps eliminate sensor blind spots and reduce trafficrelated risks. Vehicles generate HD Map data at fixed intervals, denoted as inter-packet arrival time (IPAT), while radar-sensing data is generated aperiodically, with a fixed data size. The gNodeB plays a critical role in efficiently allocating CG resources by leveraging traffic information and Channel State Information (CSI) received from vehicles. This information exchange occurs through Radio Resource Control (RRC) signaling, where vehicles report data characteristics-such as periodicity and packet size-allowing the gNodeB to make informed CG allocation decisions. To manage UL radio resource allocation, the gNodeB employs a scheduling algorithm and transmits configuration details to the vehicles via RRC messages. These include Resource Block (RB) assignments, MCS values, and the starting and ending slot indices for Type-1 CG allocations, in accordance with 5G NR specs [14]. Furthermore, the gNodeB can dynamically update RB and MCS allocations through RRC reconfiguration messages at predefined intervals (i.e., CG_w). This dynamic reallocation capability allows the system to adapt to varying UL demands, which are influenced by vehicular mobility and channel conditions, as illustrated in Fig. 1. Such adaptive scheduling of CG resources optimizes radio resource

utilization and improves communication reliability in highly dynamic vehicular networks.

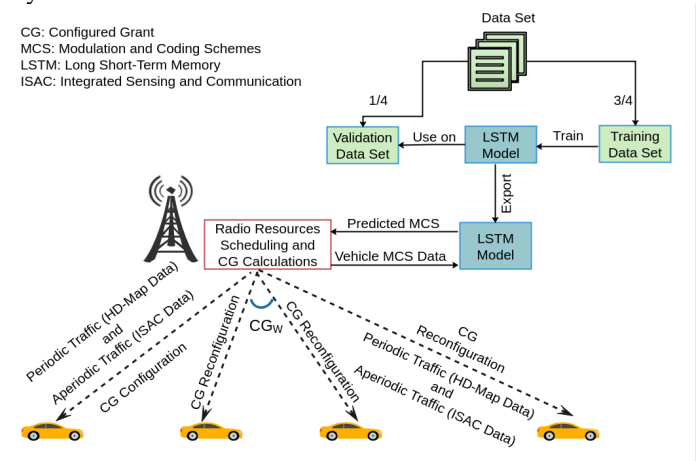


Figure 1: The training and execution process of the LSTMbased prediction module utilizes a dataset to forecast MCS values, which support the MAC scheduler in managing both HD Map data (periodic traffic) and ISAC data (aperiodic traffic). An initial CG configuration message is used to allocate CG resources, while CG reconfiguration messages periodically update transmission parameters—such as UL MCS and assigned RBs—for each vehicle at defined intervals of CG_w .

IV. CG SCHEDULING FOR SENSING DATA

This section proposes a radio resource scheduling mechanism ₂ WeibullParameters ← FitWeibullDistribution(InterArrivals) for CG allocation to minimize packet drops in vehicular environments for aperiodic ISAC traffic. The proposed Algorithms 1 and 2 model the arrival pattern of aperiodic sensing data and estimate a discrete value that approximates a pseudoperiod. The CG scheduler then uses this estimated period to allocate radio resources more effectively for sensing data transmission. Packet drops can occur because the gNodeB preassigns transmission slots for aperiodic traffic using CG. If a scheduled CG slot coincides with the arrival of an ISAC data 6 foreach t ∈ PredictedInterArrivals do packet, the transmission proceeds; otherwise, the packet may be 7 dropped due to the absence of a matching resource allocation. In this context, the parameter CG_w is crucial in balancing PDR and radio resource efficiency. A smaller CG_w may lead to more frequent reconfiguration and increased control overhead, but 9 can also result in a higher packet drop rate due to less accurate period estimation. On the other hand, a larger CG_w reduces control signaling but may cause significant resource wastage due to the allocation of unused slots. Therefore, selecting an optimal CG_w is key to maintaining high PDR while conserving radio resources.

A. Algorithm 1: Predict Aperiodic Arrival Times using Weibull Distribution

The Algorithm 1 predicts the future arrival times of aperiodic sensing events based on observed event arrivals within a defined CG_w . Algorithm 1 begins by computing the inter-arrival times (InterArrivals) as the differences between consecutive entries in the arrival list (Line 1). As demonstrated in the case study presented in [15], the Weibull distribution can effectively model the inter-arrival times of aperiodic events. Accordingly, in Line 2, the computed inter-arrival times are fitted to a Weibull distribution, and the resulting parameters are stored in WeibullParameters, capturing the statistical characteristics of the observed data. Using these parameters, the Algorithm 1 proceeds to generate the same number of predicted interarrival times as those observed (Line 4). To construct the corresponding arrival timestamps, the algorithm initializes an empty list, PredictedArrivals (Line 4), and appends the last known sensing event time from the input data (Line 5). Then, from Lines 6 to 8, the algorithm cumulatively adds the predicted inter-arrival times to the last known arrival time to obtain the future sensing event arrival times. Finally, the algorithm returns PredictedArrivals, which contains the predicted future arrival times of aperiodic sensing events. This approach leverages statistical modeling to forecast event timings based on historical data patterns.

Algorithm 1 Predicting Aperiodic Arrival Times using Weibull Distribution

```
: Arrivals = [a_1, a_2, \ldots, a_n] // Aperiodic event arrival
Input
         times for previous time window
Output : PredictedArrivals // Predicted arrival times for
```

1 InterArrivals ← CalculateDifference(Arrivals)

```
// Compute differences between consecutive arrivals
```

// Fit Weibull distribution to inter-arrival times

3 ArrivalsLength ← CalculateLength(Arrivals)

// Calculate Length of Aperiodic event

4 PredictedInterArrivals ← Predict(WeibullParameters, ArrivalsLength)

// Generate predicted inter-arrival times

5 PredictedArrivals ← Arrivals[ArrivalsLength]

// Initialize list for predicted arrival times

Last ← CalculateLength(PredictedArrivals) $PredictedArrivals \leftarrow PredictedArrivals[Last] + t$ // Append the next predicted arrival time

return PredictedArrivals

B. Algorithm 2: Find the Best Period with Allowed Thresholds

This algorithm aims to determine an efficient CG period that aligns with the majority of predicted sensing event arrivals, while satisfying two key constraints: the Hit Ratio Threshold (HitRatioThresh) and the Resource Block Wastage Threshold (RBwastageThresh). It takes as input the sensing arrival times from a previous observation window, the CG window duration, and the threshold values for hit ratio and resource block wastage. The algorithm begins by invoking Algorithm 1 on the input Arrivals data to generate the set of predicted future arrivals (PredictedArrivals) (Line 1), based on a learned model from historical data. Initially, the variable BestConfiguredGrantPeriod is set to None (Line 4), indicating that no valid period has yet been selected.

```
Algorithm 2 Computing the Best Period with Allowed Thresholds
```

```
inputs : Arrivals = [a_1, a_2, \dots, a_n], HitRatioThresh, , CG_w
                  BestConfiguredGrantPeriod
   output :
                                                    // Optimal period
             satisfying constraints
 1 PredictedArrivals ← PredictAperiodicArrival(Arrivals)
   // Predict Aperiodic Arrival Times using Weibull
   Distribution
 _{2} N \leftarrow CalculateLength(Arrivals) // Total number of events
 i \leftarrow 0 // Initialize index for alignment search
 4 BestConfiguredGrantPeriod \leftarrow None // Initialize best period
 5 AlternatePeriod ← None // Initialize Alternate Period
 6 PredictedArrivalsSet ← set(PredictedArrivals) // Convert to set
    for faster membership checks
  for period \leftarrow 1 to 9 do
         / Reset aligned count for current period
       alignedCount \leftarrow 0
           Locate the first data point aligning with the
           current period
       while i < N and (PredictedArrivals[i] mod period) \neq 0 do
        i \leftarrow i + 1
10
       if i > N then
11
           continue
                         // No aligning data point found, skip
12
             this period
       // Initialize starting point for alignment
       temp \leftarrow PredictedArrivals[i]
13
           Count aligned events (multiples of the period
           or off by 1)
       while temp \leq PredictedArrivals[N] do
14
           if \ temp \in PredictedArrivalsSet \ then
15
                alignedCount \leftarrow alignedCount + 1
16
           else if temp - 1 \in \mathsf{PredictedArrivalsSet} then
17
                alignedCount \leftarrow alignedCount + 1
18
           temp \leftarrow temp + period
19
       // Calculate metrics
       RBAllocated \leftarrow floor(\frac{CG_w}{period})
20
       \mathsf{RBLoss} \leftarrow \tfrac{\mathsf{RBAllocated} - \mathsf{alignedCount}}{\mathsf{RBAllocated}}
21
       HitRatio \leftarrow \tfrac{alignedCount}{\cdots}
22
       // Evaluate constraints for the current period
       if HitRatio \geq HitRatioThresh and RBLoss \leq then
23
           BestConfiguredGrantPeriod ← period
24
       if HitRatio > HitRatioThresh then
25
           Alternate Period \leftarrow period
   // Final selection
27 if BestConfiguredGrantPeriod = None then
       BestConfiguredGrantPeriod ← AlternatePeriod // Fallback to
        backup period
29 return BestConfiguredGrantPeriod // Return the best period
```

For faster lookup during alignment checks, *PredictedAr-rivalsSet* is initialized as a set (Line 6). A loop then iterates

over possible period values from 1 to 9 milliseconds. For each candidate period, the algorithm attempts to identify the first arrival time that aligns with it (Lines 9–10), and this aligned time is stored in the temporary variable *temp* (Line 13). Starting from this point, a while loop (Line 14) checks whether future predicted arrivals occur at integer multiples of the candidate period. Each successful match increments the *alignedCount* variable (Lines 15–16), representing the number of sensing events that can be offloaded exactly at CG transmission opportunities. Lines 17–18 extend this logic by allowing for limited buffering: if a sensing event does not align exactly with the CG slot, the algorithm permits it to be uploaded within the next scheduling slot, assuming free radio resources are available.

This improves offloading efficiency and minimizes wasted transmission opportunities. Following this, the algorithm computes performance metrics such as Resource Block Loss and Hit Ratio (Lines 20-22). If both metrics satisfy their respective threshold constraints, the current period is marked as valid (Lines 23-24) and stored as BestConfiguredGrantPeriod. If only the hit ratio meets its threshold, the current period is stored as AlternatePeriod (Lines 25-26). If no period satisfies both constraints by the end of the loop, the algorithm selects AlternatePeriod as the final BestConfiguredGrantPeriod (Lines 27–28), prioritizing hit ratio over RB efficiency. The returned period thus represents the most suitable CG interval that approximates aperiodic sensing traffic with minimal resource loss. The algorithm effectively extracts a quasi-periodic pattern from a set of aperiodic arrivals, supporting efficient CG-based scheduling. Its overall time complexity is $\mathcal{O}(n)$, where n is the number of sensing task arrivals in the observed time window.

V. SIMULATION AND PERFORMANCE EVALUATION

This section outlines the simulation environment, details the dataset used for training the LSTM model, and presents the resulting performance evaluation. It also examines the various CG allocation strategies utilized in this study.

A. Simulation Setup

As a case study, we evaluate the performance of the proposed scheme using the HD Map application and ISAC jobs within the 5G-LENA module of NS-3 [16]. The simulation is based on a highway scenario derived from real-world road segments in Winnipeg, Canada, specifically a 250-meter stretch of the two-way Pembina Highway. To generate realistic vehicular traffic patterns, we employ the Rapid Cellular Network Simulation Framework (RACE) [17], which integrates Simulation of Urban Mobility (SUMO)² and OpenStreetMap³ for mobility modeling. Additionally, real-world cellular infrastructure data provided by Canada's Innovation, Science and Economic Development (ISED) department⁴ is incorporated into the simulation. Vehicles in the simulation generate Constant Bit Rate (CBR) traffic with fixed periodicity (for HD Map App) and packet

²http://www.sumo.dlr.de/userdoc/SUMO.html

³http://www.openstreetmap.org/

⁴https://sms-sgs.ic.gc.ca/eic/site/sms-sgs-prod.nsf/eng/h_00010.html

sizes, and aperiodic traffic (for ISAC jobs) in the Uplink. The key simulation parameters are outlined in Table I. Parameters related to ISAC jobs follow the settings defined in [18], while the remaining settings are adopted from [16]. Each simulation scenario is repeated 10 times by varying seeds, and the results are reported with 95% confidence intervals. For training the LSTM model, we used the Berlin V2X dataset [19] and set the parameters according to [11].

Table I: Simulation Parameters

Parameter	Value
Number of vehicles $ \mathcal{V} $	15
Mobility model	Krauss
Average vehicle speed (V_{speed})	20 - 80 kmph
5G NR gNodeb/Vehicle TX power	46/23 dBm
5G NR gNodeb antenna tilt	15°
5G NR gNG/Vehicle antenna height	25/1.5 meter
Carrier frequency	5.9 GHz
Channel model	UMa_LoS
5G NR gNodeb antenna model	OmniDirectional
Vehicle antenna model	Isotropic
Channel bandwidth	30 MHz
5G NR numerology (μ)	1, 2
MAC scheduler	LSTM-5GL-OFDMA
	LSTM-RB-OFDMA
	SR-Based-RR
Packet Size (L) of HD Map App	60 bytes
Packet Periodicity (IPAT) of HD Map App	10 msec
Data Size (L_isac) of ISAC Jobs	[2,6] k bits
CPU cycles required to compute ISAC Jobs	[3,5] k cycles/bit
Latency Requirement of ISAC Task	23 msec
Slot Configurations	1D13U
CG Configuration Window (CG_w)	5-15 seconds
Simulation Time	50 seconds

B. Comparison Schemes

We consider the following state-of-the-art, proposed, and baseline CG radio resource scheduling schemes:

- LSTM-5GL-OFDMA: It is an enhanced version of the 5GL-OFDMA [16] scheme, where the resource allocation is guided by MCS values predicted by an integrated LSTM model.
- LSTM-RB-OFDMA: It is a variation of the RB-OFDMA [16] scheme that incorporates an LSTM-based prediction model, using the predicted MCS values to guide RB allocation.
- SR-Based-Round Robin (SR-Based-RR): It allocates a fixed number of RBs to each UE in turn, following a round-robin approach to ensure fair and equal access to the available resources.

Among the existing CG resource allocation strategies, 5GL-OFDMA and RB-OFDMA represent the current state-of-the-art approaches. In contrast, LSTM-5GL-OFDMA and LSTM-RB-OFDMA are the proposed models in this work, which integrate LSTM-based prediction to enhance scheduling efficiency. Additionally, the SR-Based-RR scheduler is employed as a baseline for comparison. The performance of these schemes is evaluated using the following metrics:

 Packet Delivery Ratio: It measures the proportion of successfully received packets relative to the total number of packets sent within the network.

- RLC delay: RLC delay refers to the time elapsed from when a packet is created at the RLC layer of the UE to when it is successfully received at the RLC layer of the gNodeB.
- Average RBs Allocation: This metric evaluates how efficiently RBs are utilized by different CG allocation schemes. It is expressed as the percentage of RBs assigned by each scheme as compared to the total RBs consumed under the SR-Based-RR scheduler.

C. Simulation Results and Analysis

1) Effect of CG_w on PDR: To analyze how the (CG_w) length affects the PDR, we varied the CG_w from 5 to 20 secs in 5 secs increments for both LSTM-5GL-OFDMA and LSTM-RB-OFDMA under the HD-Map and ISAC-Jobs workloads. Figure 2 shows the resulting PDR at a vehicle speed of $V_{speed} = 60 \ kmph$, numerology $\mu = 1$, and packet size of L = 60 bytes. PDR climbs with longer CG_w and levels off near 15 secs for both LSTM variants. The PDR increase occurs because the gNodeB, via RRC reconfiguration, adapts transmission parameters {UL MCS, RBs} more effectively when the LSTM model sees a window length that captures the prevailing channel dynamics-here, the mobility pattern of vehicles traveling at $V_{speed} = 60 \text{ kmph}$. Specifically, the LSTM predicts each vehicle's uplink MCS from its recent history; the gNodeB then allocates the required RBs based on that prediction, packet size, and periodicity. Given that the best performance appears at $CG_w \approx 15$ secs, we fix CG_w to 15 secs for the remainder of our experiments at $V_{\text{speed}} = 60 \text{ kmph}$.

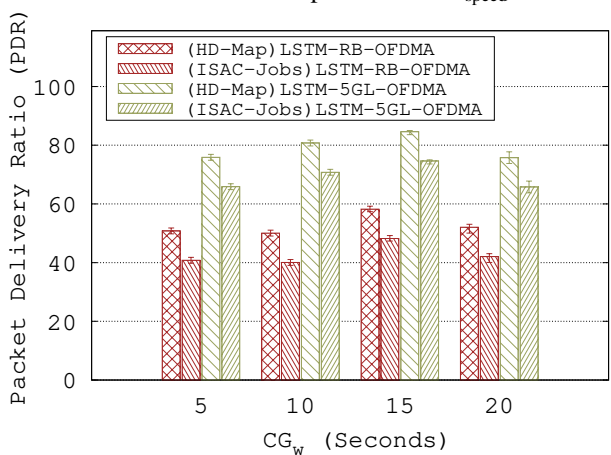


Figure 2: PDR for HD Map application and ISAC-Jobs with $\mu=1$ by varying CG_w for V=15 with $\mathcal{V}_{speed}=60$ kmph where L=60 bytes.

2) PDR and RLC delay: Figures 3(a) and 3(b) illustrate the PDR and RLC delay for the scheduling schemes LSTM-5GL-OFDMA, LSTM-RB-OFDMA, and the SR-based-RR (i.e., dynamic scheduling) under two numerologies, $\mu=1$ and $\mu=2$, with a vehicle speed of $\mathcal{V}_{speed}=60$ kmph. The performance is evaluated for both HD-Map traffic (periodic) and ISAC Jobs (aperiodic). As shown in the plots, both LSTM-5GL-OFDMA and LSTM-RB-OFDMA achieve higher PDR than their traditional counterparts, with performance approaching the SR-based-RR method. This validates the effectiveness of

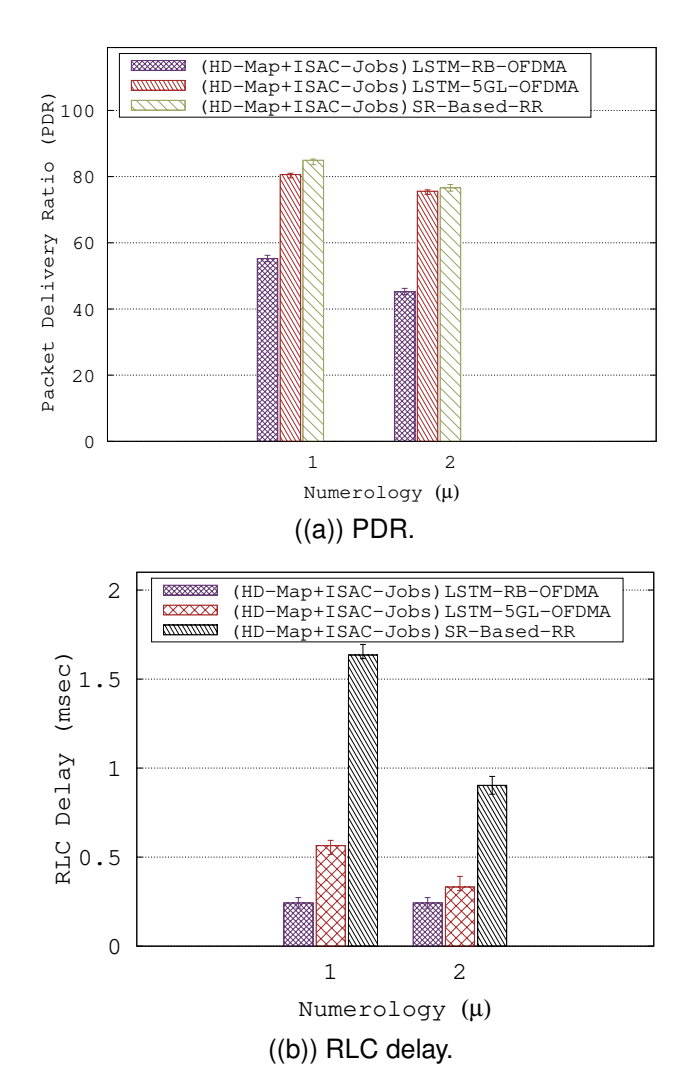
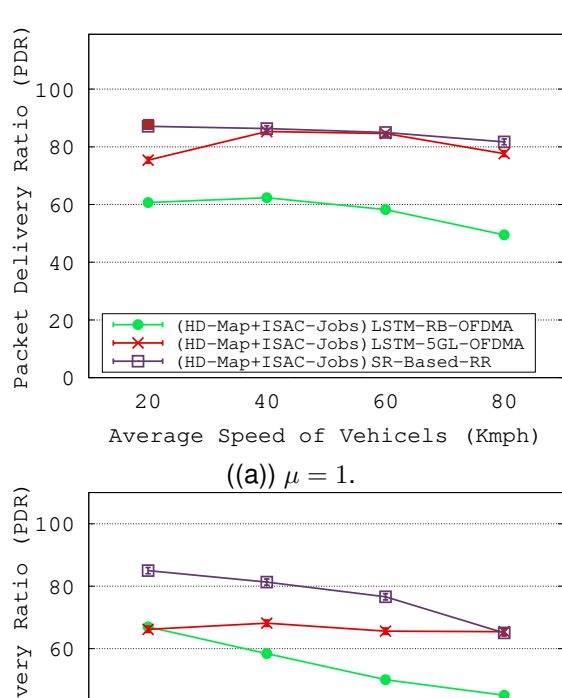


Figure 3: Result observed for HD Map application and ISAC-Jobs by varying numerology for V=15 with $\mathcal{V}_{speed}=60~kmph$ where L=60 bytes and $CG_w=15$.

predicting ISAC task arrivals using the Weibull distribution. Among the two LSTM-assisted methods, LSTM-RB-OFDMA demonstrates lower RLC delay due to its more precise and efficient resource block allocation, highlighting a trade-off between latency and delivery ratio. However, LSTM-5GL-OFDMA offers improved robustness in high-mobility scenarios, since it operates in the frequency domain, making it less sensitive to time-domain variations. This allows it to maintain a higher PDR compared to LSTM-RB-OFDMA. Although the SR-based-RR method delivers the best PDR overall, it suffers from significant RLC delays due to increased control signaling between the gNodeB and vehicles. Furthermore, all methods show a reduction in PDR for $\mu = 2$ relative to $\mu = 1$, primarily because the shorter slot duration in $\mu = 2$ leads to greater packet fragmentation. Notably, LSTM-5GL-OFDMA shows a steady improvement over LSTM-RB-OFDMA, with observed PDR gains of 14% for $\mu = 1$ and 44% for $\mu = 2$ when compared to 5GL-OFDMA.

3) Speed of vehicles: To analyze how varying vehicle speeds affect the PDR across different radio resource allocation al-



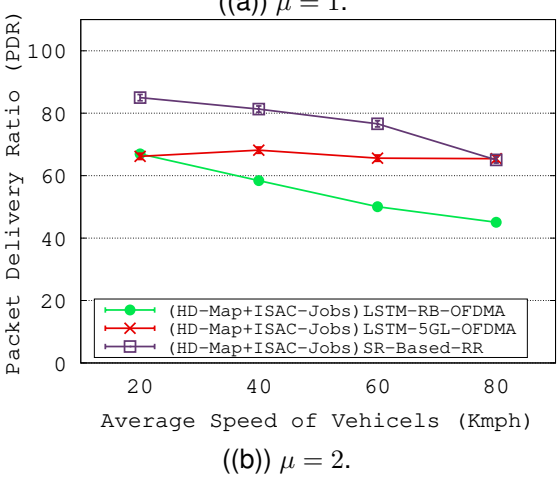


Figure 4: Result observed for HD Map application and ISAC-Jobs by varying speed of vehicles for V=15 where L=60 bytes and $CG_w=15$.

gorithms, vehicle speed is adjusted in SUMO by modifying the acceleration and maximum speed parameters. The resulting mobility traces are then imported into NS-3 to simulate different numerology settings. As illustrated in Figures 4(a) and 4(b), there is a noticeable decline in PDR as the average vehicle speed increases from $\mathcal{V}speed=20$ kmph to $\mathcal{V}speed=80$ kmph, for both $\mu=1$ and $\mu=2$, across all evaluated algorithms. Notably, LSTM-5GL-OFDMA maintains performance levels comparable to the SR-based-RR approach under both numerology settings, demonstrating its resilience under high-mobility conditions.

4) Average RBs Allocation: Figure 5 shows the average radio resource consumption of LSTM-5GL-OFDMA and LSTM-RB-OFDMA under numerologies $\mu=1$ and $\mu=2$, with a vehicle speed of $\mathcal{V}_{speed}=60$ kmph and L=60 bytes. The results indicate that LSTM-RB-OFDMA consumes approximately 20% more RBs for $\mu=1$ and 19% more for $\mu=2$ compared to LSTM-5GL-OFDMA, while offering lower RLC delay. This trade-off arises from the difference in how the two schemes allocate resources, despite both leveraging LSTM-based predictions of transmission parameters such as

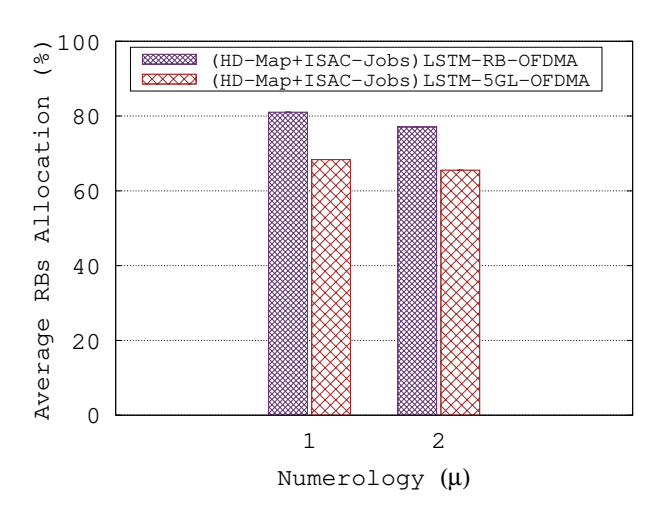


Figure 5: RBs allocation ratio with respect to SR-based-RR scheme by varying numerology for V=15 with $\mathcal{V}_{speed}=60~kmph$ where L=60 bytes and $CG_w=15$.

uplink MCS and RB requirements. These predictions also rely on modeling the arrival patterns of ISAC jobs using the Weibull distribution, which has shown to be effective in capturing aperiodic traffic behavior. Based on these predictions, the gNodeB updates transmission parameters dynamically via RRC reconfiguration messages at a periodic interval defined by the CG window ($CG_w=15$), resulting in improved efficiency in radio resource utilization.

VI. CONCLUSIONS

This paper introduced a novel approach to applying Configured Grant (CG) scheduling in Vehicle-to-Everything (V2X) networks for handling both periodic HD Map data and aperiodic sensing traffic of ISAC systems. Through a case study involving vehicles running HD Map applications alongside real-time ISAC sensing tasks, we demonstrated the need for efficient CG-based resource allocation in the uplink of 5G based V2X networks to meet the stringent latency and reliability requirements of autonomous driving applications. To support aperiodic traffic, we proposed a Weibull distribution-based CG scheduling algorithm, which models the inter-arrival times of sensing events to predict future traffic patterns using an estimate of a discrete value that approximates a pseudo-period. This estimated period is then used by the CG scheduler to allocate radio resources more effectively for sensing data transmission. Simulation results confirmed that this method improves Packet Delivery Ratio (PDR) and reduces radio resource wastage, compared to baseline and non-predictive CG strategies. This work serves as a foundational study on CG-based resource allocation for aperiodic traffic in V2X networks. Future research will focus on extending the proposed framework to support more complex and interactive use cases, such as Virtual Reality (VR) traffic, which imposes even stricter latency and reliability constraints in next-generation vehicular applications.

ACKNOWLEDGEMENT

This research work was supported by the Science and Engineering Research Board, New Delhi, India. Grant number: JBR/2021/000005.

REFERENCES

- [1] 3rd Generation Partnership Project (3GPP), "Study on Integrated Sensing and Communication (ISAC)," 2024, Rel-19. [Online]. Available: https://www.3gpp.org/ftp/Specs/archive/38_series/38.858/
- [2] —, "Study on enhancement of 3GPP support for 5G V2X services," 2020, rel-16. [Online]. Available: https://www.3gpp.org/ftp/Specs/archive/22_series/22.886/
- [3] SAE International, "Taxonomy and Definitions for Terms Related to Driving Automation Systems for On-Road Motor Vehicles," SAE Standard J3016, Apr. 2021, 2021 revision. [Online]. Available: https://www.sae.org/standards/content/j3016_202104/
- [4] J. Levinson, J. Askeland, J. Becker, J. Dolson, D. Held, S. Kammel, J. Z. Kolter, D. Langer, O. Pink, V. Pratt et al., "Towards fully autonomous driving: Systems and algorithms," in *IEEE Intelligent Vehicles Symposium* (IV). IEEE, 2011, pp. 163–168.
- [5] G. Grassi, D. Pesavento, G. Pau, R. Wakikawa, and L. Zhang, "Vanet via named data networking," in *Proceedings of IEEE INFOCOM Workshops*. IEEE, 2014, pp. 410–415.
- [6] HERE Technologies, "Hd live map: A foundation for autonomous driving," 2018, white Paper. [Online]. Available: https://www.here.com/ platform/hd-live-map
- [7] Volvo Car Group, "Volvo cars partners with here to deliver real-time data for improved road safety," 2015, press Release. [Online]. Available: https://group.volvocars.com/news/press-releases/2015/volvo-cars-partners-with-here-to-deliver-real-time-data-for-improved
- [8] Q. Liu, S. Wang, Q. Liu, and Z. Qi, "Joint computation offloading and resource allocation strategy in isac-assisted v2x networks based on mec," in 2023 International Conference on Information Processing and Network Provisioning (ICIPNP), 2023, pp. 85–89.
- [9] N. C. Luong, T. Huynh-The, T.-H. Vu, D. V. Le, H. T. Nguyen, N. D. Hai, G.-V. Nguyen, N. D. D. Anh, D. Niyato, D. I. Kim, and Q.-V. Pham, "Advanced learning algorithms for integrated sensing and communication (isac) systems in 6g and beyond: A comprehensive survey," *IEEE Communications Surveys Tutorials*, pp. 1–1, 2025.
- [10] B. Hu, W. Zhang, Y. Gao, J. Du, and X. Chu, "Multiagent deep deterministic policy gradient-based computation offloading and resource allocation for isac-aided 6g v2x networks," *IEEE Internet of Things Journal*, vol. 11, no. 20, pp. 33890–33902, 2024.
- [11] V. K. Gautam, V. R. Chintapalli, B. R. Tamma, and C. S. R. Murthy, "Exploring the feasibility of configured grant for vehicular scenario," in 2023 IEEE 98th Vehicular Technology Conference (VTC2023-Fall), 2023, pp. 1–6.
- [12] F. Marzuk, A. Vejar, and P. Cholda, "Deep reinforcement learning for energy-efficient 6g v2x networks," *Electronics*, vol. 14, no. 6, p. 1148, 2025.
- [13] Y. Cang, M. Chen, and Z. Yang, "Cooperative detection for mec aided multi-static isac systems," in 2024 IEEE 100th Vehicular Technology Conference (VTC2024-Fall), 2024, pp. 1–6.
- [14] 3GPP, "NR; NG-RAN Overall Description," *Release 16, (TS) specication* 38.300, V16.7.0, 2021.
- [15] D. A. Khan, N. Navet, B. Bavoux, and J. Migge, "Aperiodic traffic in response time analyses with adjustable safety level," in *Proc. IEEE Inter*national Conference on Emerging Technologies and Factory Automation (ETFA), Palma, Spain, Sep. 2009.
- [16] A. Larrañaga, M. C. Lucas-Estañ, S. Lagén, Z. Ali, I. Martinez, and J. Gozalvez, "An open-source implementation and validation of 5G NR configured grant for URLLC in ns-3 5G LENA: A scheduling case study in industry 4.0 scenarios," *Journal of Network and Computer Applications*, vol. 215, p. 103638, 2023.
- [17] F. e. a. Jomrich, "Demo: rapid cellular network simulation framework for automotive scenarios (race framework)," in *Proc. of International Conference on Networked Systems (NetSys)*, 2017, pp. 1–2.
- [18] Y. Zhao, F. Hou, J. Huang, B. Lin, and H. Shan, "Delay optimization in vehicular edge computing with sensing information fusion and heterogeneous tasks," in 2024 IEEE International Conference on Communications Workshops (ICC Workshops), 2024, pp. 1888–1894.
- [19] R. Hernangómez, P. Geuer, A. Palaios, D. Schäufele, C. Watermann, K. Taleb-Bouhemadi, M. Parvini, A. Krause, S. Partani, C. Vielhaus et al., "Berlin V2X: A machine learning dataset from multiple vehicles and radio access technologies," arXiv preprint arXiv:2212.10343, 2022.